# CREEP BOWING IN CANDU FUEL: MODELLING AND APPLICATIONS[$]

S.D. YU*, M. TAYAL**, Z. XU**

*Department of Mechanical Engineering, Ryerson Polytechnic University
Toronto, Ontario, Canada M5B 2K3

**Atomic Energy of Canada Ltd.
2251 Speakman Drive, Mississauga, Ontario, Canada L5K 1B2

## ABSTRACT

This paper outlines a new capability that has been added to the BOW code, namely, to assess creep-induced bowing. Good agreement was obtained between the code and independent analytical solutions for creep bending of beams. Illustrative examples of creep bowing of CANDU® fuel are also given.

## INTRODUCTION

During irradiation, lateral deflection (bowing) of a fuel element occurs because of in-service temperatures and external loads (Veeder and Schankula 1974). On-power bowing and sheath distortions need to be kept reasonably low in order to ensure that the fuel bundle can be easily removed from the reactor, and to preclude the possibility of impairing the heat transfer from the sheath or overheating the pressure tube or both. To date, bowing has not caused any operational difficulty in any CANDU power plant. Assessments of elastic and creep bowing of fuel elements can help demonstrate the integrity of nuclear fuel and its surrounding components.

The BOW code (Tayal 1989, Yu and Tayal 1995) calculates the bowing of a fuel element consisting of sheath, pellets and appendages. The driving forces considered in the code are temperature gradients, hydraulic drag, and gravity. The fuel element is subjected to restraint from endplates, neighbouring fuel elements and the pressure tube. The finite element method is used to assess element bow under normal operating conditions as well as during dryout that lasts for a few seconds.

Post-irradiation measurements have shown that creep in the reactor increases bowing significantly (Veeder and Schankula 1974). A capability to calculate creep deflections has now

---

[$]Presented at the Fifth International Conference on CANDU Fuel, Canadian Nuclear Society, Toronto, Canada. 1997 September 21-25.

® CANDU is a registered trademark of Atomic Energy of Canada Limited (AECL).

been added to the BOW code, and is described in this paper. The total displacement of the sheath caused by external loads and creep is calculated for each node at each time step. The cumulative strain for the entire duration is calculated by summing the appropriate components from the individual time steps. This paper describes the following aspects of assessing creep-induced bowing: mathematical modelling, algorithms and comparisons with independent results. Illustrative applications of the creep bowing calculations in the design assessments of nuclear fuel are also discussed.

## MATHEMATICAL DESCRIPTION

A fuel element may be modelled as a three dimensional composite beam supported by the two endplates and limited by pressure tube and neighbouring fuel elements. A finite beam element is shown in Figure 1, where $x$, $y$ and $z$ represent the horizontal, vertical and axial directions, respectively; the $z$ axis passes through the centroid of beam cross section; u, v and w represent the three displacements in the $x$, $y$ and $z$ directions; $\theta_x$ and $\theta_y$ are the two angles of rotation measured in the $xoz$ and $yoz$ planes; subscripts 1 and 2 are the two local node numbers of a three-dimensional finite beam element. In developing the BOW code, we used the following assumptions:

- The lateral deflection of the beam (fuel element) is small.
- The applied loads are quasi-static; or the applied loads are either independent of time or vary slowly with time so that inertia effects may be ignored.
- Plane cross-sections perpendicular to the z-axis remain plane, which is consistent with the Euler elastic beam theory.
- Effect of shear deformation is negligible.

From the above assumptions and Hooke's law, the stress and the total axial strain at a material point $(x, y, z)$, may be expressed as

$$\varepsilon_z = \varepsilon_z^e + \varepsilon_z^c = \lambda(z) - \kappa_x(z)x - \kappa_y(z)y \tag{1}$$

$$\sigma_z = E(\varepsilon_z - \varepsilon_z^c) = E(\lambda - \kappa_x x - \kappa_y y - \varepsilon_z^c) \tag{2}$$

where definitions of all mathematical symbols used in this paper are given in the nomenclature section. From the above equations, the resultant bending moments and axial force may be written as

$$M_x = \iint_A \sigma_z x dA = -E\left(I_y\kappa_x + I_{xy}\kappa_y\right) - M_x^c \tag{3}$$

$$M_y = \iint_A \sigma_z y dA = -E\left(I_x\kappa_y + I_{xy}\kappa_x\right) - M_y^c \tag{4}$$

$$N_z = \iint_A \sigma_z dA = EA\lambda - N_z^c \tag{5}$$

At time $t$, the following equations of equilibrium may be obtained by considering the resultant forces in the $x$, $y$ and $z$ directions:

$$\frac{\partial^2 M_x}{\partial z^2} + N_z \frac{\partial^2 u}{\partial z^2} + q_x = 0, \quad \frac{\partial^2 M_y}{\partial z^2} + N_z \frac{\partial^2 v}{\partial z^2} + q_y = 0, \quad \frac{\partial N_z}{\partial z} + q_z = 0 \tag{6}$$

In the BOW code, the distributed load in the axial direction, which may be caused by the viscous or frictional forces, is negligible. Therefore, the axial force resultant is a constant and equal to the hydraulic drag. Equation (6) is then reduced to

$$\frac{\partial^2 M_x}{\partial z^2} - P \frac{\partial^2 u}{\partial z^2} + q_x = 0, \quad \frac{\partial^2 M_y}{\partial z^2} - P \frac{\partial^2 v}{\partial z^2} + q_y = 0 \tag{7}$$

The displacements and kinetically admissible arbitrary displacements within a beam element may be defined in terms of the nodal displacements as

$$u = [N_x]^e \{\delta_x\}^e, \quad v = [N_y]^e \{\delta_y\}^e, \quad u^* = [N_x]^e \{\delta_x^*\}^e, \quad v^* = [N_y]^e \{\delta_y^*\}^e \tag{8}$$

Multiplying Equation (7) by two weighted functions, $u^*$ and $v^*$, and integrating over the entire element length $l_e$, we obtain the following equations of equilibrium for a finite beam element

$$\begin{bmatrix} K_{xx} & K_{xy} \\ K_{yx} & K_{yy} \end{bmatrix}^e \begin{Bmatrix} \delta_x \\ \delta_y \end{Bmatrix}^e = \begin{Bmatrix} P_x \\ P_y \end{Bmatrix}^e + \begin{Bmatrix} P_x^c \\ P_y^c \end{Bmatrix}^e \text{ or } [K]^e \{\delta\}^e = \{P\}^e + \{P^c\}^e \tag{9}$$

where the creep-induced load matrices are defined as

$$\{P_x^c\}^e = -\int_0^{l_e} \{[B_x]^e\}^T M_x^c dz, \quad \{P_y^c\}^e = -\int_0^{l_e} \{[B_y]^e\}^T M_y^c dz$$

Equation (9) describes how each individual finite element deforms in response to its applied loads. To determine the overall deformation of the entire fuel element, the responses of all the individual finite elements need to be summed to form the following global equations of equilibrium:

$$[K]\{\delta\} = \{P\} + \{P^c\} \tag{10}$$

Various types of creep laws have been developed to model the creep behaviour of engineering materials. The commonly used creep laws include the Norton power law (Hult 1966), strain-hardening law, and the time-dependent Graham-Walles law (Freed and Alexander 1967). For

Zircaloy, creep laws accounting for the effect of stress, strain, temperature, irradiation and microstructure have been developed at AECL and elsewhere in the nuclear industry. The current version of the BOW code accommodates power laws and power laws with strain-hardening effect.

During creep bending, the neutral axis of pure bending may not coincide with the centroid of the cross-section area. It can be shown (Shames and Cozzarelli 1992) that the neutral axis lies between the centroid and the median of the cross-section area. However, if the cross-section area is doubly symmetric with respect to the $x$ and $y$ axes, the neutral axis is identical to that for the linear elastic bending because the axis of centroid coincides with the median axis. For a nuclear fuel element having pellets, bearing pads and spacer pads, the neutral axis of creep bowing is different from that of elastic bowing.

In general, the creep rate is a non-linear function of local stress and strain. As well, the creep deflection increases the moment arm for the hydraulic drag load, which in turn increases the local stress and thus results in additional creep. Because of the above non-linearities and feedbacks, the following incremental approach is adopted in the BOW code for solving Equation (10) for elastic-creep analyses: (a) calculate elastic deflection at the end of $t = 0$; (b) update the stiffness matrix and load matrix, determine the creep-induced load, and calculate the deflection at the end of $t = t + \Delta t$; and (c) continue step (b) until desired time period has been reached. The procedure may be best described by the following hierarchical equations:

$$[K]\{\delta\}_0 = \{P\}_0;\ [K]\{\delta\}_1 = \{P\}_1 + \{P^c\}_1;\ \ldots;\ [K]\{\delta\}_t = \{P\}_t + \{P^c\}_t;\ \ldots \qquad (11)$$

The incentive to develop the above creep model stemmed from immediate applications to creep of fuel elements, as described in more detail later. Nevertheless, the above derivation shows that the creep model is completely general, and can be easily adapted to other components of the fuel bundle such as endplates.

## CONVERGENCE

The mid-interval time difference scheme, also called the Crank-Nicholson scheme (Hsu 1986), was implemented in the BOW code, to improve the accuracy in the calculation of creep strain and stress redistribution at every material point.

One of the important parameters in the creep analysis is the size of the time increment. Smaller time increments are desired in all typical creep calculations, in order to achieve reasonable accuracy. However, excessively small time increments may significantly increase the computing time. To determine an optimum balance between accuracy and cost, a convergence test is conducted for a cantilever beam subjected to a concentrate load at the free end. The beam is made of non-linear viscous material defined by the following power law: $\dot{\varepsilon}_z^c = \left(\sigma_z / 6.34 \times 10^{10}\right)^3$. The flexural rigidity of the beam is $EI = 23.19\ Nm^2$. Figure 2 shows the total displacement at the free

end after 1000 h under a concentrated load of 2 N. Results shown in the figure indicate that a time increment of about 50 h provides a reasonable balance between accuracy (of 1%) and cost.

## COMPARISON WITH ANALYTICAL SOLUTIONS

Two test cases were used to verify the above method of creep calculations. They are described in detail in Table 1. For case 1, the results presented in Figure 3 indicate that the BOW calculations are in excellent agreement with the analytical solution. The differences are less than 1%. For case 2, the average difference in the maximum creep-induced deflection between the analytical solution and BOW is about 10%. The larger difference is believed to be caused by the simplifying assumptions in the analytical formulation, especially regarding the effect of stress redistribution during creep (Freed and Seyna 1965).

## ILLUSTRATIVE APPLICATIONS

To date, bowing has not caused any operational difficulty in any CANDU power reactor. We checked whether the calculations of the BOW code are consistent with the above experience. Also, we sought to quantify the operating margin in existing CANDU 6 fuel with respect to on-power bowing.

In CANDU power reactors, fuel bundles rest inside horizontal channels. Gravitational forces tend to have the largest influence on the direction of post-irradiated element bow (Dennier et al. 1996). This occurs by means of two competing mechanisms, element sag and bundle droop. Sag caused by gravity tends to bow the fuel element downwards. Therefore, bowing in the radial direction at midplane of outer elements is usually inward for the upper elements (near 12 o'clock), and outward for the lower elements (near 4 o'clock and near 8 o'clock). In the bottom elements, bundle droop results in element bowing to generally inward. Figure 5 shows the bundle profile at midplane in an irradiated fuel bundle from a Bruce B reactor (D. Dennier et al. 1996).

The calculated on-power bundle profile at the midplane of CANDU 6 fuel is shown in Figure 6. Elements near the top bow inwards (downwards) because of element sag; elements near 4 o'clock and 8 o'clock positions bow outwards. These trends are similar to those noted by Dennier et al. - see Figure 5. A more detailed review of calculated on-power clearances confirmed that no problems are expected with respect to overheating of CANDU 6 fuel or pressure tubes, or removal of CANDU 6 fuel. This is consistent with the CANDU 6 operating experience noted earlier.

## CONCLUSIONS

A model for creep bowing has been added to the BOW code. Because the finite element method is used, a number of complicating factors such as contacts, bearing pads, varying material properties can be easily modelled. Although to date the model has been tested only for creep

bowing of fuel elements, the model is versatile, and can be easily adapted to other parts of the fuel bundle such as endplates. Comparisons with independent analytical solutions show that the model is accurate.

Applications of the BOW code show that the calculations of the code are consistent with measurements on experimental irradiated fuel and with operating experience to date on CANDU 6 fuel. Sample calculations have enabled us to quantify the margins available in CANDU 6 fuel with respect to bowing and attendant consequences such as bundle removal and coolability.

## ACKNOWLEDGEMENTS

The authors gratefully acknowledge the contributions of K. Chaudhary in providing independent solutions for testing of the creep package of the BOW code. We also thank Daljit Rattan for his review, and J.H.K. Lau for his encouragement, support and review.

## REFERENCES

D. Dennier, A.M. Manzer, M.A. Ryz and E. Kohn 1995 "Characteristics of CANDU Fuel Bundles That Caused Pressure Tube Fretting at the Bundle Midplane", Presented at the16th Annual CNS Conference, Saskatoon, Saskatchwan.

D. Dennier, A.M. Manzer, M.A. Ryz and E. Kohn 1996 "Element Bow Profiles from New and Irradiated CANDU Fuel Bundles", Presented at the 17th Annual CNS Conference, Fredericton, New Brunswick.

N.H. Freed and F. Seyna 1965 "Small Deflection Creep Buckling of Magnesium Alloy (Magnox AL80) at 295°C," *Journal of Mechanical Engineering Science.* 7(3), 328-334.

N.H. Freed and J.M. Alexander 1967 "Creep Buckling of Columns with Lateral Restraint," *Journal of Strain Analysis* 2(2), 137-51.

Tai-Ran Hsu 1986 *The Finite Element Methods in Thermomechanics*, Allen & Unwin, Winchester, Mass.

J.A. Hult 1966 *Creep in Engineering Structures*, Blaisdell Publishing Company, New York, NY.

F.K. Odqvist 1966 *Mathematical Theory of Creep and Creep Rupture*, Oxford at the Clarendon Press.

I.R. Shames and F.A. Cozzarelli 1992 *Elastic and Inelastic Stress Analysis*, Prentice Hall, Englewood Cliffs, NJ.

M. Tayal 1989 "Modelling The Bending/Bowing of Composite Beams Such As Nuclear Fuel: The BOW Code", *Nuclear Engineering and Design* 116, 149-159.

S.D. Yu and M. Tayal 1995 "Improvement and Verification of BOW Code," Presented at the 4th International Conference on CANDU Fuel, Canadian Nuclear Society, Pembroke, Ontario.

J. Veeder and M.H. Schankula 1974 "Bowing of Pelletized Fuel Elements: Theory and In-Reactor Experiments", *Nuclear Engineering and Design* 29, 164-179.

NOMENCLATURE

| | |
|---|---|
| A | cross-section area |
| $[B_x]^e$ | strain-displacement function matrix |
| $[B_y]^e$ | strain-displacement function matrix |
| $I$ | second moment of area |
| $[K]$ | global stiffness matrix |
| $[K]^e$ | simultaneous element stiffness matrix |
| $l_e$ | length of a finite beam element |
| E | Young's modulus |
| $M_x$ | total bending moment in the *xoz* co-ordinate plane |
| $M_y$ | total bending moment in the *yoz* co-ordinate plane |
| $M_x^c$ | creep-induced bending moment in the *xoz* co-ordinate plane $(= \iint_A E\varepsilon_z^c x dA)$ |
| $M_y^c$ | creep-induced bending moment in the *yoz* co-ordinate plane $(= \iint_A E\varepsilon_z^c y dA)$ |
| $N_z$ | total axial resultant force |
| $N_z^c$ | creep-induced axial resultant force $(= \iint_A E\varepsilon_z^c dA)$ |
| $[N_x]^e$ | shape function matrix in the *xoz* co-ordinate plane |
| $[N_y]^e$ | shape function matrix in the *yoz* co-ordinate plane |
| $P$ | axial drag load |
| $\{P\}$ | global load matrix |
| $\{P\}^e$ | element load matrix, |
| $\{P\}_i$ | global load matrix at the end of *i*-th time step |
| $\{P^c\}^e$ | creep-induced element load matrix |
| $\{P^c\}$ | creep-induced global load matrix |
| $\{P^c\}_i$ | creep-induced global load matrix at the end of *i*-th time step |
| $\{P_x\}^e$ | nodal force vector in the *xoz* co-ordinate plane |
| $\{P_y\}^e$ | nodal force vector in the *yoz* co-ordinate plane |

| | |
|---|---|
| $\{P_x^c\}^e$ | creep-induced nodal loads in the *xoz* co-ordinate plane |
| $\{P_y^c\}^e$ | creep-induced nodal loads in the *yoz* co-ordinate plane |
| $q_x, q_y, q_z$ | distributed loads in the $x$, $y$ and $z$ directions |
| t | time |
| $u, v, w$ | displacements of a material point in the $x$, $y$ and $z$ directions, respectively |
| $u^*, v^*$ | arbitrary, kinetically admissible displacements in the $x$ and $y$ directions, respectively |
| $x, y, z$ | co-ordinates |
| $\{\delta\}$ | global nodal displacement matrix |
| $\{\delta\}^e$ | simultaneous element displacement matrix |
| $\{\delta\}_i$ | global nodal displacement matrix at the end of $i$-th time step |
| $\{\delta_x^*\}^e$ | arbitrary, kinetically admissible nodal displacement in the *xoz* co-ordinate plane |
| $\{\delta_y^*\}^e$ | arbitrary, kinetically admissible nodal displacement in the *yoz* co-ordinate plane |
| $\varepsilon_z$ | total strain at a material point $(x, y, z)$ in the axial direction |
| $\varepsilon_z^e$ | elastic strain at a material point $(x, y, z)$ in the axial direction |
| $\varepsilon_z^c$ | creep strain at a material point $(x, y, z)$ in the axial direction |
| $\theta_x, \theta_y$ | angles of rotation in the *xoz* and *yoz* planes, respectively |
| $\kappa_x$ | the curvatures measured in the *xoz* co-ordinate plane |
| $\kappa_y$ | the curvatures measured in the *yoz* co-ordinate plane |
| $\lambda$ | strain at $x = 0$ and $y = 0$ in the axial direction |
| $\sigma_z$ | stress at a material point $(x, y, z)$ in the axial direction |

Table 1 Description of Test Cases

| Cases | Descriptions | Creep laws and Parameters | Developer |
|---|---|---|---|
| 1 | A cantilever beam 500 mm long, subjected to a concentrated lateral load of 2 N applied at the free end. | $\dot{\varepsilon} = \left(\frac{\sigma}{6.34 \times 10^{10}}\right)^3$ <br> $EI = 23.19\, Nm^2$ | Odqvist (1966) |
| 2 | A simply supported beam 500 mm long, subjected to axial load of 400 N. The initial deflection profile is sinusoidal. | $\dot{\varepsilon} = \left(\frac{\sigma}{1.49 \times 10^{18}}\right)$ <br> $EI = 23.19\, Nm^2$ <br> $v_o = 0.1 \sin(\pi z / l)$ | Freed and Seyna (1965) |

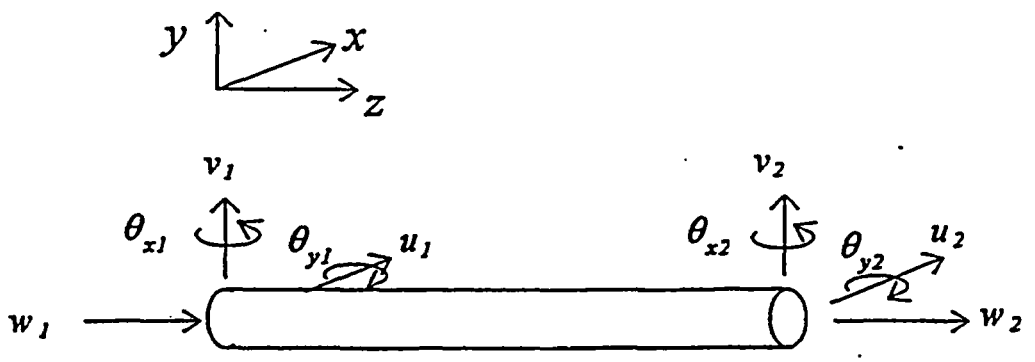


Figure 1 A FINITE BEAM ELEMENT IN THREE DIMENSION

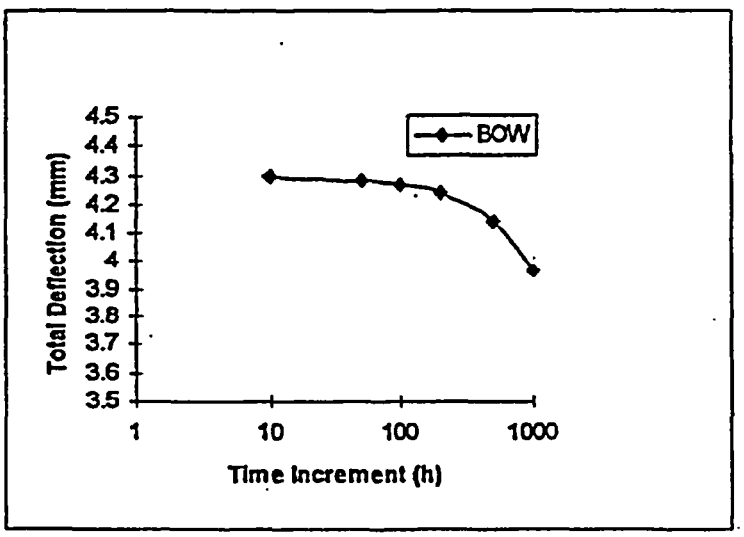


Figure 2 TOTAL DEFLECTION AT THE FREE END VS. TIME INCREMENT

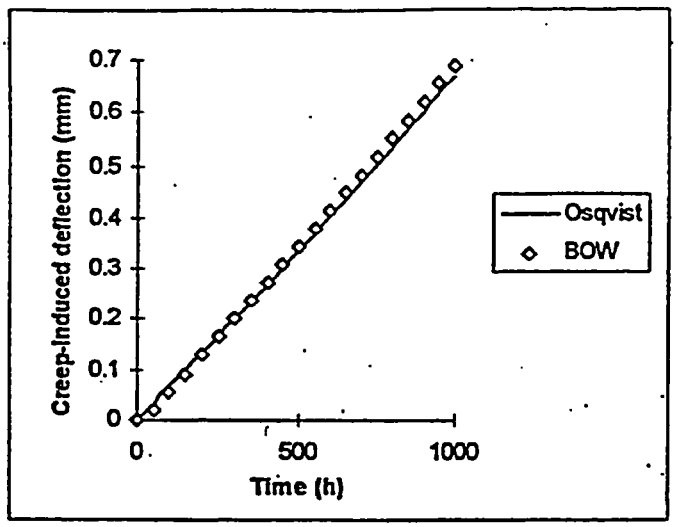


Figure 3 CREEP DEFLECTION AT THE FREE END OF CANTILEVER BEAM

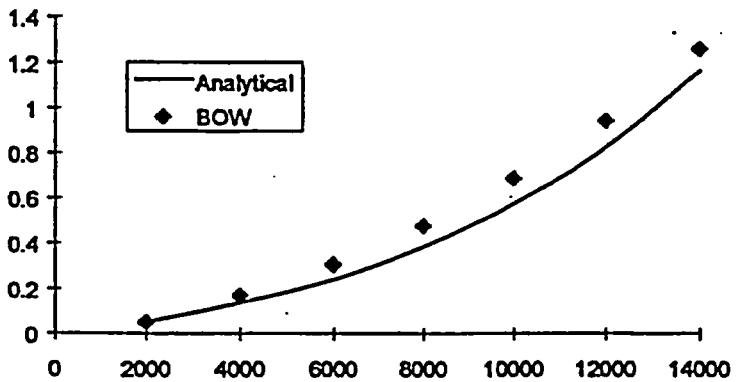


Figure 4 CREEP DEFLECTION AT THE CENTRE OF A SIMPLY SUPPORTED BEAM

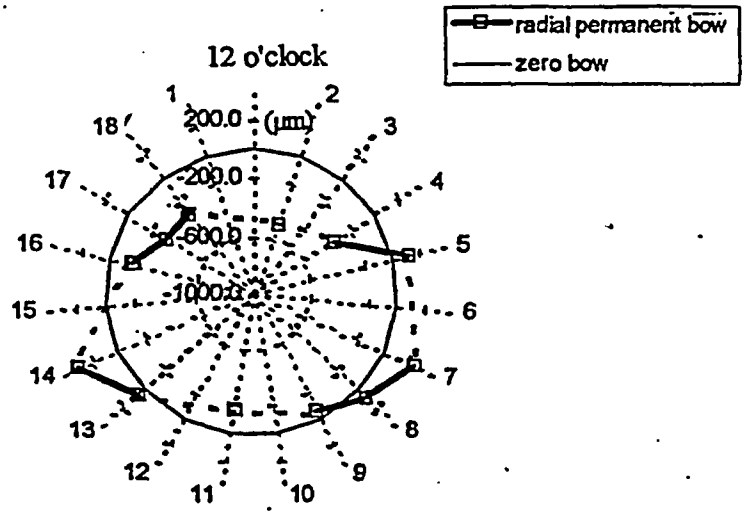


Figure 5 MEASURED PERMANENT BOW IN AN IRRADIATED BRUCE BUNDLE

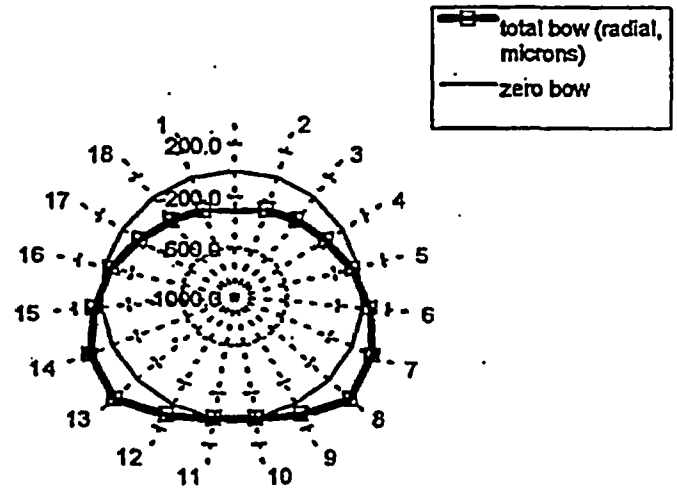


Figure 6 PREDICTED IN-REACTOR RADIAL BOW AT MIDPLANE OF CANDU 6 OUTER ELEMENTS

Canadian Nuclear Society

FIFTH INTERNATIONAL CONFERENCE ON CANDU FUEL

CANDU FUEL: BUILDING ON EXCELLENCE

CANDU FUEL: BUILDING ON EXCELLENCE

CANDU FUEL: BUILDING ON EXCELLENCE

CANDU FUEL: BUILDING ON EXCELLENCE

CANDU FUEL: BUILDING ON EXCELLENCE

September 21-25, 1997

# CONFERENCE PROCEEDINGS Vol. 1

Vol. 1: ISBN 0-919784-48-8
Set: ISBN 0-919784-50-X

Cameco Corporation

CANDU Owners Group

GE Canada Nuclear Products

IAEA

Zircatec Precision Industries Inc.